Available online at www.sciencedirect.com
SCIENCE DIRECT®
Journal of Solid State Chemistry 178 (2005) 3507–3513
JOURNAL OF SOLID STATE CHEMISTRY
www.elsevier.com/locate/jssc

Synthesis of Sm^{3+}-doped strontium barium niobate crystals in glass by samarium atom heat processing

Nakorn Chayapiwut, Tsuyoshi Honma, Yasuhiko Benino, Takumi Fujiwara, Takayuki Komatsu*

Department of Chemistry, Nagaoka University of Technology, 1603-1 Kamitomioka-cho, Nagaoka 940-2188, Japan

Received 6 July 2005; received in revised form 29 August 2005; accepted 6 September 2005
Available online 3 October 2005

Abstract

New glasses giving the crystallization of Sm^{3+}-doped $Sr_xBa_{1-x}Nb_2O_6$ (SBN) ferroelectrics have been developed in the Sm_2O_3–SrO–BaO–Nb_2O_5–B_2O_3 system, and the formation of SBN crystal dots and lines by continuous wave Nd:YAG laser (wavelength:1064 nm, power: 1 W) irradiations, i.e., samarium atom heat processing, has been examined. The formation of Sm^{3+}-doped SBN non-linear optical crystals is confirmed from X-ray diffraction analyses, micro-Raman scattering spectra, second harmonic generations, and photoluminescence spectra. Sm^{3+}-doped SBN crystal dots with the diameters of 20–70 μm and lines with the widths of 20–40 μm are written at the surface of some glasses such as $10Sm_2O_3 \cdot 10SrO \cdot 10BaO \cdot 20Nb_2O_5 \cdot 50B_2O_3$ (mol%) by Nd:YAG laser irradiations with the irradiation times of 20–70 s for the dots and with the scanning speeds of 1–5 μm/s for the lines. The present study suggests that the samarium atom heat processing has a potential for the patterning of optical waveguides consisting of ferroelectric SBN crystals in glass substrates.

Keywords: Laser-induced crystallization; Glasses; SBN crystals; Photoluminescence; Raman scattering spectra

1. Introduction

Strontium barium niobates, $Sr_xBa_{1-x}Nb_2O_6$ (hereafter referred to as SBN) with $0.25 \leqslant x \leqslant 0.75$, are well-known crystals with a tetragonal tungsten-bronze structure and possess various excellent ferroelectric and non-linear optical properties such as extremely large electro-optic coefficients [1–3]. It is, however, known that the growth of bulk SBN single crystals is difficult [4]. It has been desired to develop SBN thin films with optical waveguide functions for integrated optic devices [5]. On the other hand, recently, laser irradiation has been recognized as a process for spatially selected structural modifications in glass, and three-dimensional channels (structural damages with refractive index changes) have been micromachined in silica glasses by femtosecond laser pulse irradiations [6–8]. Considering that glass has been widely used in telecommunication network systems, the direct patterning of optical waveguides consisting of ferroelectric/nonlinear optical crystals such as SBN in glass would have advantages compared with the use of single crystals such as $LiNbO_3$.

Recently, the present authors' group [9–13] succeeded in forming crystal dots and lines in Sm_2O_3 (or Dy_2O_3)-containing glasses by continuous wave (cw) Nd: yttrium–aluminum–garnet (YAG) laser (wavelength of $\lambda = 1064$ nm) irradiations. For instance, $Sm_xBi_{1-x}BO_3$ and β'-$Sm_2(MoO_4)_3$ crystal lines showing second harmonic generations (SHGs) have been written in Sm_2O_3–Bi_2O_3–B_2O_3 and Sm_2O_3–MoO_3–B_2O_3 glasses by YAG laser irradiations. In this processing, cw Nd:YAG lasers with $\lambda = 1064$ nm are absorbed by Sm^{3+} in glass through f–f transitions ($^6F_{9/2} \leftarrow {}^6H_{5/2}$) and the surrounding of Sm^{3+} is heated through a non-radiative relaxation (electron–phonon coupling). Consequently, structural modifications (refractive index changes) or crystallizations are induced. This technique for the direct writing of crystal dots and lines in glass is called "samarium atom heat processing"

*Corresponding author. Fax: +81 258 47 9300.
E-mail address: komatsu@chem.nagaokaut.ac.jp (T. Komatsu).

0022-4596/$ - see front matter © 2005 Elsevier Inc. All rights reserved.
doi:10.1016/j.jssc.2005.09.002

[9,11]. It is of importance to demonstrate that this unique crystal growth processing is applicable to the writing of various functional crystals in glass.

In this study, we focus our attention on the formation of SBN ferroelectrics in glass, and in particular, the writing of SBN crystal dots and lines by Nd:YAG laser irradiations has been tried. New glasses giving the formation of SBN non-linear optical crystals have been developed in the Sm_2O_3–SrO–BaO–Nb_2O_5–B_2O_3 system, i.e., the pseudo-ternary Sm_2O_3–SBN–B_2O_3 system, and it has been confirmed that the samarium atom heat processing is working for the writing of SBN crystal dots and lines in this glass system.

2. Experimental

The Sm_2O_3–SrO–BaO–Nb_2O_5–B_2O_3 glasses were prepared using a conventional melt quenching method. The glass compositions examined in this study are given in Table 1. Commercial powders of reagent grade Sm_2O_3, $SrCO_3$, $BaCO_3$, Nb_2O_5, and B_2O_3 were mixed and melted in a platinum crucible at 1400 °C for 1 h in an electric furnace. The melts were poured onto an iron plate and pressed to a thickness of about 1.5 mm with another iron plate. Glass transition, T_g, crystallization onset, T_x, crystallization peak, T_p, and melting, T_m, temperatures were determined using differential thermal analyses (DTA) at a heating rate of 10 K/min. Densities of the glasses, d, were measured with the Archimedes method using kerosene as an immersion liquid. Refractive indices, n, were measured at room temperature using an ellipsometer at a wavelength of 632.8 nm. Optical absorption spectra were measured in the wavelength range of 190–3200 nm using a spectrometer.

The glasses were heat treated at various temperatures for 1 h in an electric furnace, and crystalline phases present in the heat-treated samples were examined using X-ray diffraction (XRD) analyses (Cu$K\alpha$ radiation) at room temperature. Second harmonic (SH) intensities of the crystallized glasses were measured by using a fundamental wave of a Q-switched Nd^{3+}: YAG laser at $\lambda = 1064$ nm. The powder method proposed by Kurtz and Perry [14] was applied, and pulverized α-quartz particles were used as a reference.

The glasses were mechanically polished to a mirror finish with CeO_2 powders and were exposed to cw Nd^{3+}:YAG lasers with $\lambda = 1064$ nm. The YAG lasers with a power of 1 W were focused at the surface of the glasses using an objective lens (60 ×), and the glasses were moved by a computer-controlled stage. The translation speeds of the stage were 1–20 μm/s. Crystal dots and lines were observed with a polarization optical microscope and examined from the measurements of micro-Raman scattering and photoluminescence spectra (Tokyo Instruments Co., Nanofinder; Ar^+ laser 488 nm).

3. Results and discussion

3.1. Search for new glasses giving SBN crystallization

For the purpose of the present study, firstly we searched new glasses giving the formation of SBN crystals by the crystallization in an electric furnace (i.e., conventional crystallization). So far, it has been reported that the SrO–BaO–Nb_2O_5–TeO_2 and SrO–BaO–Nb_2O_5–SiO_2 glasses give SBN ferroelectrics by a conventional crystallization [15,16]. In this study, i.e., in the samarium atom heat processing, it is a key point to explore new glasses containing some amounts of Sm_2O_3. Considering that borate glasses have a good ability for a large solubility of rare-earth oxides as a general trend, we examined the Sm_2O_3–SrO–BaO–Nb_2O_5–B_2O_3 system. As a result, it was found that some glasses can be prepared in this system using a conventional melt-quenching method and SBN crystals can be formed through the crystallization of those glasses. It is known that the ferroelectric properties of $Sr_xBa_{1-x}Nb_2O_6$ crystalline phases depend on the Sr/Ba ratio. In this study, we focus our attention on the $Sr_{0.5}Ba_{0.5}Nb_2O_6$ phase (hereafter referred to as SBN) as a typical example, and, therefore, make a target on glasses

Table 1
Glass compositions, the values of glass transition temperature, T_g, crystallization onset temperature, T_x, crystallization peak temperature, T_p, melting temperature, T_m, density, d, and refractive index, n, for Sm_2O_3–SrO–BaO–Nb_2O_5–B_2O_3 glasses

Glass (mol%)					T_g (°C)	T_x (°C)	T_p (°C)	T_m (°C)	d (g/cm^3)	n
Sm_2O_3	SrO	BaO	Nb_2O_5	B_2O_3	(±2)	(±2)	(±2)	(±2)	(±0.01)	(±0.02)
5	11.25	11.25	22.5	50	606	688	707	912		
7	7.5	7.5	15	63	599	705	737	880	3.78	1.77
8	7.5	7.5	15	62	609	701	735	875	3.86	1.78
8	8.75	8.75	17.5	57	631	760	794	895	3.73	1.80
8	10	10	20	52	614	708	758	875	4.20	1.85
10	5	5	10	70	635	724	749	890		
10	6.25	6.25	12.5	65	622	715	737	891		
10	7.5	7.5	15	60	619	699	742	835	4.05	1.81
10	8.75	8.75	17.5	55	623	718	751	858	4.24	1.85
10	10	10	20	50	626	712	727	876	4.41	1.87
10	11.25	11.25	22.5	45	633	745	769	892		

with the nominal composition of $Sr_{0.5}Ba_{0.5}Nb_2O_6$ such as $10Sm_2O_3 \cdot 10SrO \cdot 10BaO \cdot 20Nb_2O_5 \cdot 50B_2O_3$, i.e., SrO/BaO = 1 and $Nb_2O_5/(SrO + BaO) = 1$. The proper amount of Sm_2O_3 in glass for the synthesis of crystals using YAG laser irradiations has been found to be around 8 mol% as reported in the previous papers [9–13]. The glasses with the Sm_2O_3 contents of 5–10 mol% were, therefore, prepared. In this paper, for simplification, we use Sm_2O_3–SBN–B_2O_3 as the description for the glass compositions. For example, the description of $10Sm_2O_3 \cdot 40SBN \cdot 50B_2O_3$ (mol%) means the composition of $10Sm_2O_3 \cdot 10SrO \cdot 10BaO \cdot 20Nb_2O_5 \cdot 50B_2O_3$ (mol%).

The nominal compositions of the glasses prepared in this study are shown in Table 1. The glasses with the contents of 5–10 mol% Sm_2O_3, 20–45 mol% SBN, and 45–70 mol% B_2O_3 were successfully prepared. The DTA patterns for some glasses are shown in Fig. 1, indicating the endothermic peaks due to the glass transition and exothermic peaks due to the crystallization. The values of T_g, T_x, T_p, and T_m determined from the DTA curves are summarized in Table 1. It is seen that the glasses developed in this study have the values of 599–635 °C for T_g, 688–760 °C for T_x, 707–794 °C for T_p, and 835–912 °C for T_m. All glasses have relatively large differences ($\Delta T = T_x - T_g$: 80–129 °C) between T_x and T_g, indicating that the glasses have a good thermal stability against crystallization. It should be pointed out that we can not prepare any clear glass samples in the composition of $45SBN \cdot 55B_2O_3$ containing no Sm_2O_3. This means that the addition of some amounts of Sm_2O_3 to the SBN–B_2O_3 system improves the glass-forming ability. The values of d and n for some glasses are given in Table 1. These glasses have the values of 3.78–4.41 g/cm^3 for density and 1.77–1.87 for refractive index. It is clear that both values increase with increasing Sm_2O_3 or SBN content. The optical absorption spectrum in the wavelength range of 850–1750 nm for the $8Sm_2O_3 \cdot 40SBN \cdot 52B_2O_3$ glass is shown in Fig. 2. It is seen that this glass has the absorption coefficient of $\alpha = 5.29\,cm^{-1}$ at 1064 nm for the *f–f* transition of $^6H_{5/2} \rightarrow {}^6F_{9/2}$ in Sm^{3+} ions. This value is almost the same as that ($\alpha = 6.48\,cm^{-1}$) for the $10Sm_2O_3 \cdot 30Bi_2O_3 \cdot 60B_2O_3$ glass [10], and thus we can expect that Nd:YAG laser irradiated spots in the Sm_2O_3–SBN–B_2O_3 glasses would be heated.

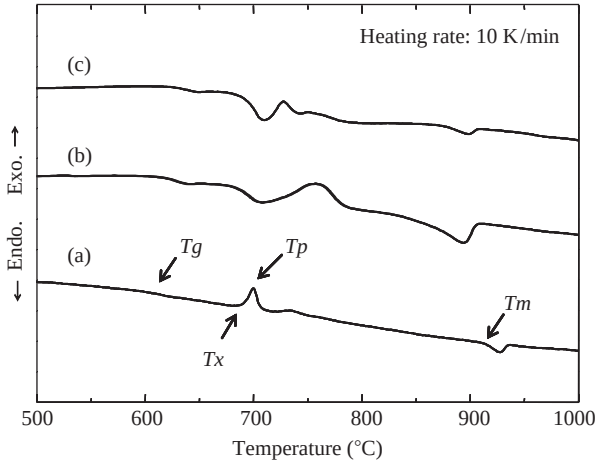

Fig. 1. DTA patterns for (a) $5Sm_2O_3 \cdot 45SBN \cdot 50B_2O_3$, (b) $8Sm_2O_3 \cdot 40SBN \cdot 52B_2O_3$, and (c) $10Sm_2O_3 \cdot 40SBN \cdot 50B_2O_3$ glasses. The heating rate was 10 K/min.

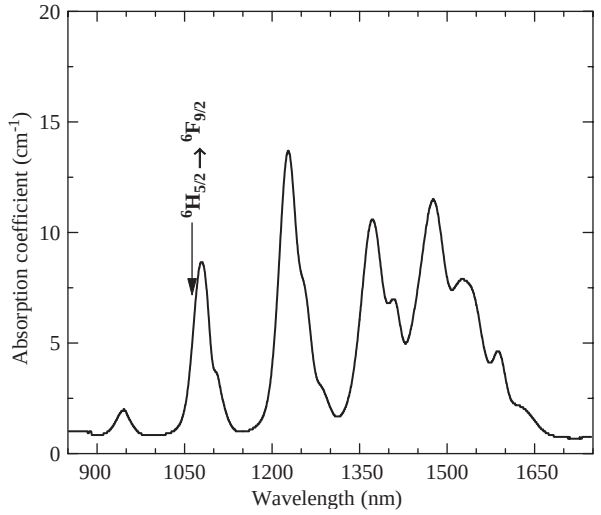

Fig. 2. Optical absorption spectrum at room temperature for $8Sm_2O_3 \cdot 40SBN \cdot 52B_2O_3$ glass.

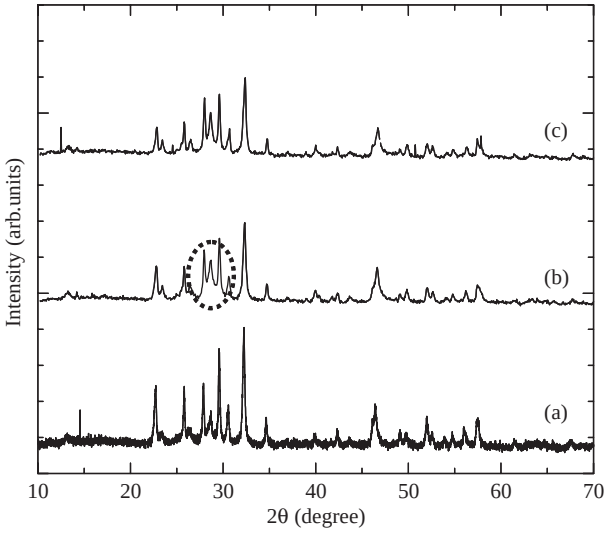

Fig. 3. XRD patterns for the crystallized glasses obtained by heat-treatment at the crystallization peak temperatures for 3 h: (a) $5Sm_2O_3 \cdot 45SBN \cdot 50B_2O_3$, (b) $8Sm_2O_3 \cdot 40SBN \cdot 52B_2O_3$, (c) $10Sm_2O_3 \cdot 40SBN \cdot 50B_2O_3$.

The powder XRD patterns for some crystallized glasses obtained by heat-treatment at T_p for 3 h are shown in Fig. 3. The peaks are assigned to the SBN crystalline phase with a tetragonal tungsten-bronze structure. In the $5Sm_2O_3 \cdot 45SBN \cdot 50B_2O_3$ crystallized glass, the sharp peaks are observed and there is no indication about the presence of other phases besides the SBN phase. The lattice constants estimated from the XRD peaks are $a = 1.247$ and $c = 0.3935$ nm and are well consistent with the reported values ($a = 1.246$ and $c = 0.3952$ nm in JCPDS.

No. 39–265, $a = 1.247$ and $c = 0.394$ nm in Ref. [17]) for the $Sr_{0.5}Ba_{0.5}Nb_2O_6$ phase. These results suggest that the Sr/Ba ratio in the $Sr_xBa_{1-x}Nb_2O_6$ crystals formed in the crystallized glass of $5Sm_2O_3 \cdot 45SBN \cdot 50B_2O_3$ might be close to Sr/Ba = 1, i.e., $Sr_{0.5}Ba_{0.5}Nb_2O_6$. The SHG was clearly observed in the crystallized sample of $5Sm_2O_3 \cdot 45SBN \cdot 50B_2O_3$, and its intensity, $I^{2\omega}$, was approximately 11 times as large as = -quartz powders, i.e., $I^{2\omega}$ (crystallized glass)/$I^{2\omega}$ (α-quartz) = 11. It is, therefore, clear that the SBN crystals present in this crystallized glass are nonlinear optical crystals. The Curie temperature of $Sr_{1-x}Ba_xNb_2O_6$ crystals with $x = 0.2-0.8$ is 60–250 °C [18,19], and SHGs have been reported in some researchers [3,20].

In the crystallized glasses of $8Sm_2O_3 \cdot 40SBN \cdot 52B_2O_3$ and $10Sm_2O_3 \cdot 40SBN \cdot 50B_2O_3$, the peaks appeared at $2\theta = 27-30^\circ$ are overlapped each other compared with those for the $5Sm_2O_3 \cdot 45SBN \cdot 50B_2O_3$ crystallized glass as shown in Fig. 3 (the overlapped region is marked by a dotted circle). These results imply that the formation of SBN crystals is affected by the amount of Sm_2O_3 in the precursor glasses. It is known that rare-earth (RE^{3+}) ions such as Nd^{3+} are incorporated into SBN crystals [17,21]. Considering the ionic radii of Ba^{2+} (0.136 nm), Sr^{2+} (0.113 nm) and RE^{3+} (~0.10 nm), rare-earth ions might be mainly substituted at the site of Sr^{2+} in SBN crystals [22–24]. It is noted that the XRD patterns for the crystallized samples of $8Sm_2O_3 \cdot 40SBN \cdot 52B_2O_3$ and $10Sm_2O_3 \cdot 40SBN \cdot 50B_2O_3$ shown in Fig. 3 are very similar to that of $Ba_{0.66}Er_{0.22}Nb_2O_6$ crystals with a tungsten bronze structure reported by Sakamoto et al. [24]. It is, therefore, considered that some amounts of Sm^{3+} are incorporated into the SBN crystals formed in the crystallized glasses with large amounts (8–10 mol%) of Sm_2O_3. The SHGs were observed in the fully crystallized samples with 8–10 mol% Sm_2O_3, but their intensities were small, i.e., $I^{2\omega}$ (crystallized glass)/$I^{2\omega}$ (α-quartz) = 1–2. The Curie temperature of $Sr_{0.5}Ba_{0.5}Nb_2O_6$ single crystals has been reported to be 120 °C [18]. It is, however, known that the Curie temperature of SBN crystals is lowered by rare-earth doping [25]. The small SH intensities in our samples might indicate the formation of Sm^{3+}-doped SBN crystals. The incorporation of Sm^{3+} into SBN crystals will be again discussed in the next section. In our preliminary study on the P (polarization)-E (electric field) relation at room temperature, hysteresis loops, i.e., remanent polarization, were observed for the $5Sm_2O_3 \cdot 45SBN \cdot 50B_2O_3$, $8Sm_2O_3 \cdot 40SBN \cdot 52B_2O_3$, and $10Sm_2O_3 \cdot 40SBN \cdot 50B_2O_3$ crystallized glasses, supporting that the SBN crystals formed in these crystallized glasses are ferroelectrics at room temperature [26].

3.2. Synthesis of SBN crystals by YAG laser irradiation

As indicated in the previous section, the Sm_2O_3-SBN(SrO + BaO + Nb_2O_5)–B_2O_3 glasses are good precursors for the formation of SBN crystals through the crystallization. The Nd:YAG laser irradiation experiments were, therefore, carried out for some Sm_2O_3-SBN-B_2O_3 glasses. Nd:YAG lasers with a power of 1 W were irradiated at the surface of the $8Sm_2O_3 \cdot 40SBN \cdot 52B_2O_3$ and $10Sm_2O_3 \cdot 40SBN \cdot 50B_2O_3$ glasses. During the irradiation, the glass plates were heated to around 450 °C, because it was difficult to induce the crystallization by laser irradiations without heating the glass plates. It should be pointed out that the temperature of 450 °C is far below compared with the glass transition temperature (T_g = 614, 626 °C) of these glasses. That is, it is considered that the heating of the glass plates to 450 °C just assists the YAG laser-induced crystallization. In the $5Sm_2O_3 \cdot 45SBN \cdot 50B_2O_3$ glass, no significant structural changes were induced by YAG laser irradiations with a power of 1 W. The Sm_2O_3 content of 5 mol% would be small for the temperature increase in the laser irradiated spots.

The polarization optical microphotographs for the laser-irradiated samples of $10Sm_2O_3 \cdot 40SBN \cdot 50B_2O_3$ are shown in Figs. 4 and 5, where the laser irradiation times for the formation of the dots were 4 and 70 s and the laser scanning speeds for the lines were 1, 5, and 10 μm/s. The formation of a spherical dot with the size (diameter) of ~70 μm is observed at the surface of the sample irradiated for 70 s ((b) in Fig. 4). In the laser-irradiated sample of 4 s ((a) in Fig. 4), the spherical dot consists of the different phases showing different refractive indices, i.e., the black color and white color parts. From the micro-Raman scattering spectra (will be shown later), it was confirmed that the black color parts at the center of the dot shown in the optical microphotographs are crystals, e.g., SBN. In the writing of lines, it is seen that the structural change depends strongly on the scanning speed. As decreasing scanning speed, more homogeneous structures have been constructed. That is, in the line written at the speed of 10 μm/s ((c) in Fig. 5), the crystals (black part regions) are separated, but in the case of the speed of 1 μm/s ((a) in Fig. 5), the laser-irradiated part was fully crystallized. Similar results were obtained for the $8Sm_2O_3 \cdot 40SBN \cdot 52B_2O_3$ glass. The present study, therefore, indicates that the low laser scanning speeds are needed for the writing of SBN crystal lines; <1 μm/s for the $8Sm_2O_3 \cdot 40SBN \cdot 52B_2O_3$ glass and <5 μm/s for the $10Sm_2O_3 \cdot 40SBN \cdot 50B_2O_3$ glass. Furthermore, the present study suggests that the growth rate of the SBN crystals in the Sm_2O_3-SBN-B_2O_3 glasses under Nd:YAG laser irradiations is not so high. Consequently, in this study, it was demonstrated that the crystal dots with the diameters of 20–70 μm and crystal lines with the widths of 20–40 μm are written at the surface of the glasses by the samarium atom heat processing.

The micro-Raman scattering spectra for the spherical dot and line are shown in Fig. 6. For the glass (non-irradiated) part ((a) in Fig. 4), a broad peak is observed at ~800 cm^{-1}. On the other hand, for the center (black color part) of the spherical dot ((b) in Fig. 4), some peaks with strong intensities are observed; the sharp peaks at 325 and

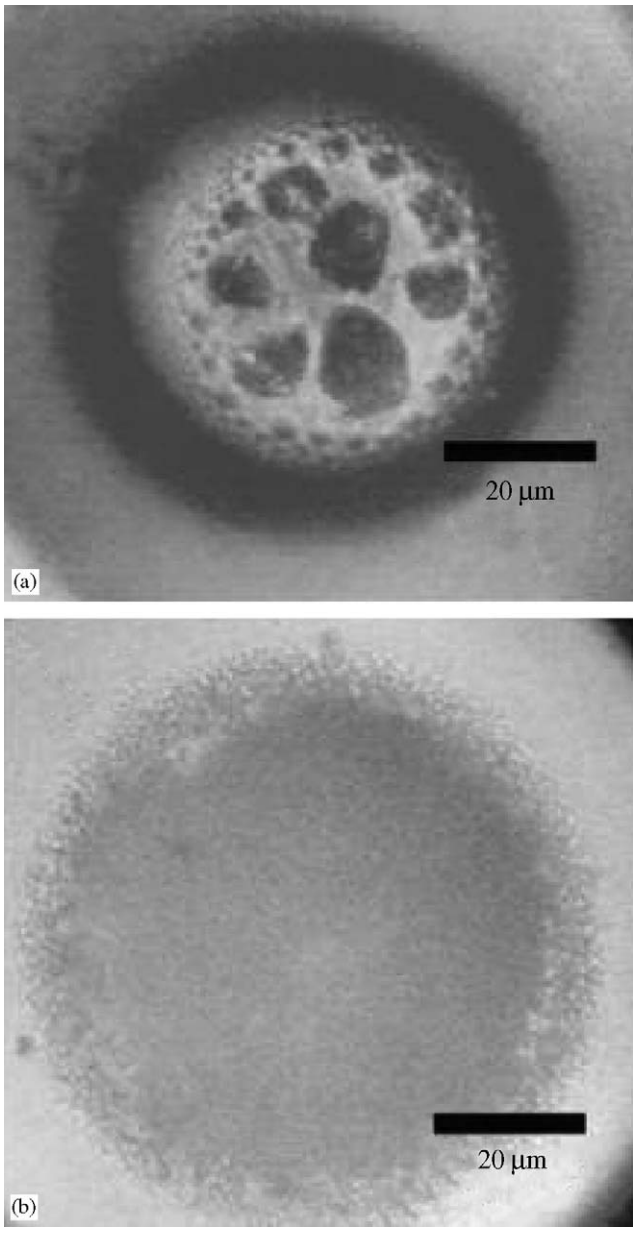

Fig. 4. Polarization optical microphotographs for the samples (dots) obtained by YAG laser irradiations (power: 1 W) in the $10Sm_2O_3 \cdot 40SBN \cdot 50B_2O_3$ glass. The laser irradiation times are 4 s for (a) and 70 s for (b).

803 cm^{-1} and the broad peak at 627 cm^{-1}. The Raman scattering spectra for $Sr_xBa_{1-x}Nb_2O_6$ crystals have been reported by several researchers [27–29]. The most prominent feature in the Raman scattering spectra for SBN crystals is a broad peak (A_1(TO) phonon) at 630–640 cm^{-1}. The broad peak at ~630 cm^{-1} shown in Fig. 6, therefore, indicates the formation of SBN crystals. That is, we can say that SBN crystals are formed in the Sm_2O_3–SBN–B_2O_3 glasses by Nd:YAG laser irradiations. It is seen that the Raman scattering spectrum for the center of the line ((c) in Fig. 4) is almost the same as that for the dot, meaning that the line written by YAG laser irradiations also consists of SBN crystals.

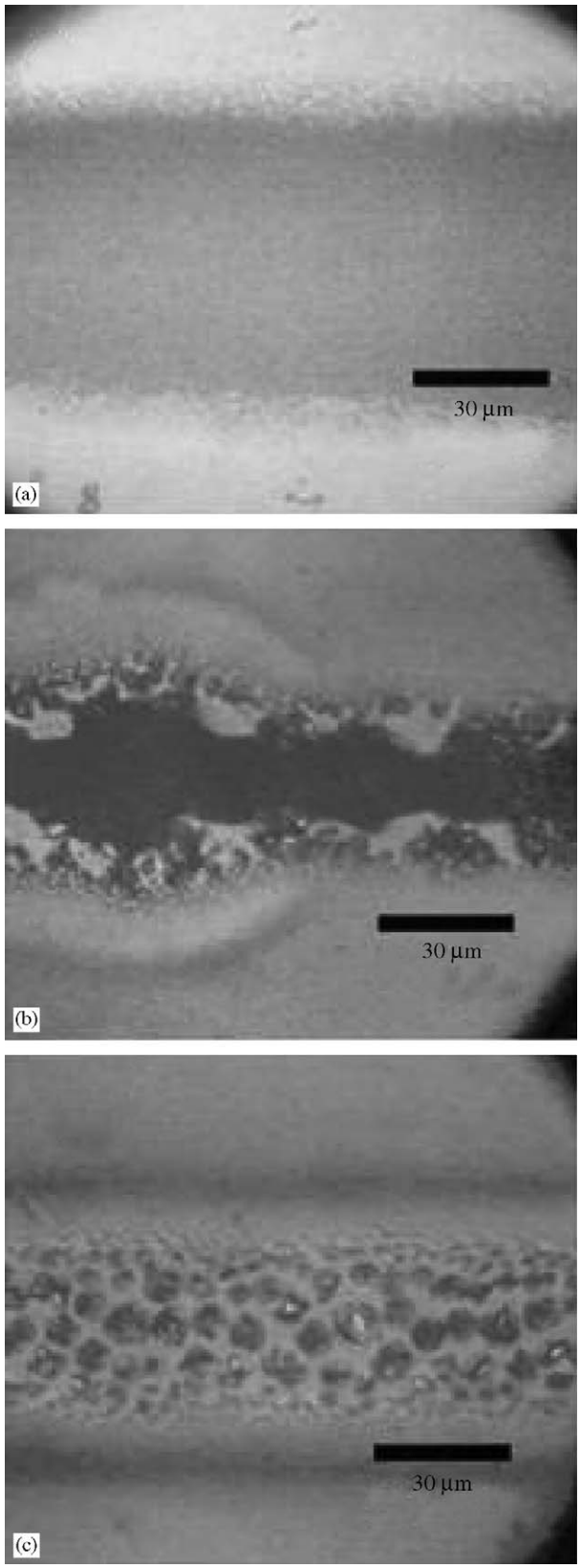

Fig. 5. Polarization optical microphotographs for the samples (lines) obtained by YAG laser irradiations (power: 1 W) in the $10Sm_2O_3 \cdot 40SBN \cdot 50B_2O_3$ glass. The laser scanning speeds are 1 μm/s for (a), 5 μm/s for (b) and 10 μm/s for (c).

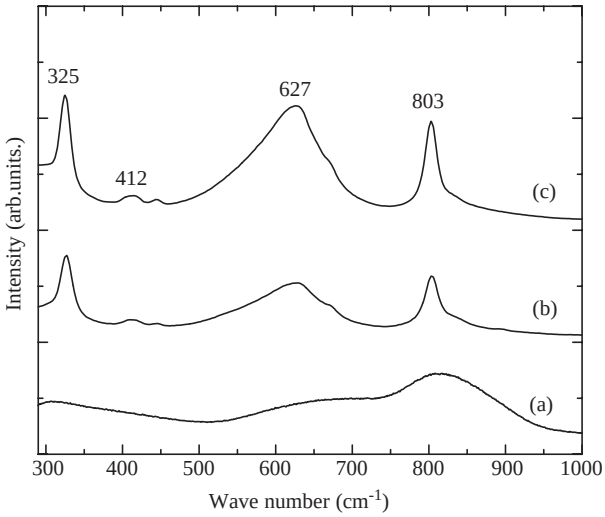

Fig. 6. Micro-Raman scattering spectra for the glass and YAG laser irradiated samples of $10Sm_2O_3 \cdot 40SBN \cdot 50B_2O_3$: (a) the glass part, (b) the center of the dot, (c) the center of the line.

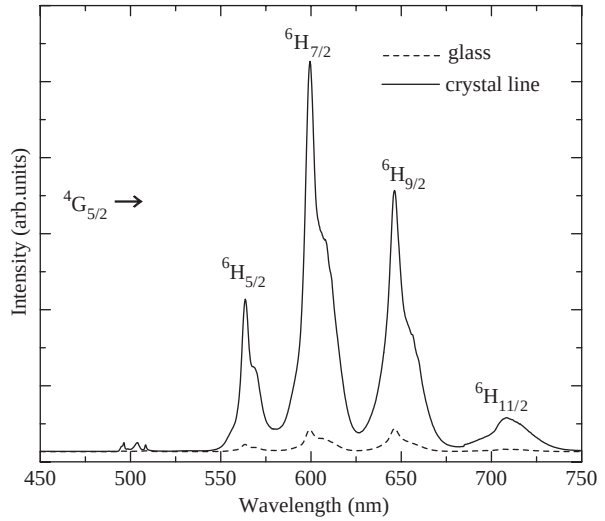

Fig. 7. Micro-photoluminescence spectra for the glass part and crystal line written by YAG laser irradiations in the $10Sm_2O_3 \cdot 40SBN \cdot 50B_2O_3$ glass.

The micro-photoluminescence spectra in the wavelength of 450–750 nm for the glass part and crystal line written by YAG laser irradiations are shown in Fig. 7. Ar^+ lasers with $\lambda = 488$ nm were used as an excitation light. As seen in Fig. 7, four luminescence peaks are observed at around 565, 600, 650, 705 nm in each sample. These are typical emission spectra of Sm^{3+}; $^4G_{5/2} \rightarrow {}^6H_{5/2}$ at 565 nm, $^4G_{5/2} \rightarrow {}^6H_{7/2}$ at 600 nm, $^4G_{5/2} \rightarrow {}^6H_{9/2}$ at 645 nm, $^4G_{5/2} \rightarrow {}^6H_{11/2}$ at 705 nm [30]. Since there is no peaks at ~683 nm ($^5D_0 \rightarrow {}^7F_0$), 725 nm ($^5D_0 \rightarrow {}^7F_2$), 760 nm ($^5D_0 \rightarrow {}^7F_3$) attributing to Sm^{2+} [31], samarium ions exist as trivalent Sm^{3+} in both the glass part and crystal line. That is, there is no indication about the valence change in samarium ions from 3+ to 2+ during cw Nd:YAG laser irradiations with a power of 1 W. As seen in Fig. 7, the intensities of the peaks in the crystal line are extremely larger than those in the glass part, suggesting that Sm^{3+} ions are incorporated into the SBN crystal lines formed by YAG laser irradiations, e.g., Sm^{3+}-doped SBN crystals. The four luminescence peaks in Fig. 7 are, however, broad, giving no clear Stark splittings. As reported by Romero et al. [32], broad photoluminescence peaks have been observed in Nd^{3+}-doped $Sr_{0.6}Ba_{0.4}Nb_2O_6$ crystals as a result of the high disorder of the crystal. SBN crystals are affected by significant intrinsic disorders, as shown by several structural investigations [33], and such a structure would give different surroundings for each rare-earth ion. Furthermore, it is considered that charge compensation mechanisms in the substitution of trivalent rare-earth ions for divalent Sr or Ba ions contribute to additional surroundings [32]. Such a structural feature in rare-earth doped SBN crystals would be the reason for the appearance in the broad photoluminescence peaks as shown in Fig. 7. The chemical analysis of the crystal dots and lines written by YAG laser irradiations in this study is now under consideration.

In the samarium atom heat processing, some amounts of cw Nd:YAG lasers with $\lambda = 1064$ nm are absorbed by Sm^{3+} in glass through *f–f* transitions and the surrounding of Sm^{3+} is heated through a non-radiative relaxation [9–13]. Therefore, the temperature of YAG laser irradiated parts in glass depends strongly on the amount of Sm^{3+}, laser power, laser irradiation time, specific heat and thermal conductivity of a given glass. Furthermore, crystallization by YAG laser irradiations will depend on the temperature and viscosity of laser-irradiated parts, and the free energy barrier for the formation of crystal nucleus (embryo). Eventually, the growth of crystals in YAG laser-induced crystallizations would be controlled by diffusions of constituent ions [10]. At this moment, the kinetics of the nucleation and crystal growth of SBN crystals in the Sm_2O_3–SBN–B_2O_3 glasses has not been clarified. In this study, for the preparation of the Sm_2O_3–SBN–B_2O_3 glasses, a large amount (45–70 mol%) of B_2O_3 is added. B_2O_3 is a typical glass-forming oxide, but is not a constituent oxide in SBN crystals. It is considered that the presence of a large amount of B_2O_3 affects largely the kinetics of the nucleation and crystal growth of SBN crystals in the Sm_2O_3–SBN–B_2O_3 glasses. That is, the presence of B_2O_3 affects arrangements and diffusions of Sr^{2+}, Ba^{2+} and Nb^{5+} for the formation of SBN crystals during YAG laser irradiations. In these points of view, good selections of the system and chemical composition of glass would be very important for the writing of crystal lines in the samarium atom heat processing. In this sense, the development of new glasses containing a small amount of glass-forming oxides is strongly desired.

Laser irradiation of glass is one of the recent topics in glass science and technology, where most of the target glasses are SiO_2-based glasses and source lasers are mainly short-wavelength excimer lasers or femtosecond-pulsed lasers. It should be emphasized that the laser used in the

samarium atom heat processing is Nd:YAG laser, which is very conventional compared with other kinds of lasers such as femtosecond-pulsed lasers. The present study, i.e., the success in synthesizing of SBN crystals, proposes that the samarium atom heat processing is expected to be a new technique for materials processing in solid state chemistry.

4. Conclusion

The glasses giving the crystallization of SBN ferroelectrics were developed in the Sm_2O_3–SrO–BaO–Nb_2O_5–B_2O_3 system, and SBN crystal dots and lines were formed at the surface of some glasses such as $8Sm_2O_3 \cdot 10SrO \cdot 10BaO \cdot 20Nb_2O_5 \cdot 52B_2O_3$ and $10Sm_2O_3 \cdot 10SrO \cdot 10BaO \cdot 20Nb_2O_5 \cdot 50B_2O_3$ by continuous wave Nd:YAG laser (wavelength:1064 nm, power: 1 W) irradiations, i.e., the samarium atom heat processing. The Sm^{3+}-doped SBN crystal dots with the diameters of 20–70 μm and lines with the widths of 20–40 μm were written at the surface of some glasses such as $10Sm_2O_3 \cdot 10SrO \cdot 10BaO \cdot 20Nb_2O_5 \cdot 50B_2O_3$ (mol%) by Nd:YAG laser irradiations. The present study suggests that the samarium atom heat processing has a potential for the patterning of optical waveguides consisting of ferroelectric SBN crystals in glass substrates.

Acknowledgments

This work was supported from Ministry of Internal Affairs and Communications Strategic Information and Communications R&D Promotion Programs (SCOPE), Grant-in-Aid for Scientific Research from the Ministry of Education, Science, Sports, Culture and Technology, Japan, and by the 21st Century Center of Excellence (COE) Program in Nagaoka University of Technology. The author (T. Komatsu) would like to thank The Mitsubishi Foundation and The Tanigawa Heat Technology Foundation for the partial financial support to this work.

References

[1] P.V. Lenzo, E.G. Spencer, A.A. Ballman, Appl. Phys. Lett. 11 (1967) 23.
[2] M.D. Ewbank, R.R. Neurgaonkar, W.K. Cory, J. Feinberg, J. Appl. Phys. 62 (1987) 374.
[3] M. Horowitz, A. Bekker, B. Fischer, Appl. Phys. Lett. 62 (1993) 2619.
[4] G.A. Rakuljio, A. Yarw, R.R. Neurgaonkar, Opt. Eng. 25 (1986) 121.
[5] S.B. Xiiong, Z.M. Ye, X.Y. Chen, X.L. Guo, S.N. Zhu, Z.G. Liu, C.Y. Lin, Y.S. Jin, Appl. Phys. A 67 (1998) 313.
[6] Y. Kondo, J. Qiu, T. Mitsuya, K. Hirao, T. Yoko, Jpn. J. Appl. Phys. 38 (1999) L1146.
[7] A. Marcinkevicius, S. Juodkazis, M. Watanabe, M. Miwa, S. Matsuo, H. Misawa, J. Nishii, Opt. Lett. 26 (2001) 277.
[8] Y. Li, K. Itoh, W. Watanabe, K. Yamada, D. Kuroda, J. Nishii, Y. Jiang, Opt. Lett. 26 (2001) 1912.
[9] T. Honma, Y. Benino, T. Fujiwara, T. Komatsu, R. Sato, Appl. Phys. Lett. 82 (2003) 892.
[10] S. Kawasaki, T. Honma, Y. Benino, T. Fujiwara, R. Sato, T. Komatsu, J. Non-Cryst. Solids 325 (2003) 61.
[11] T. Honma, Y. Benino, T. Fujiwara, T. Komatsu, R. Sato, Appl. Phys. Lett. 83 (2003) 2796.
[12] M. Abe, Y. Benino, T. Fujiwara, T. Komatsu, R. Sato, J. Appl. Phys. 97 (2005) 123516.
[13] T. Komatsu, R. Ihara, Y. Benino, T. Fujiwara, Proc. SPIE 5723 (2005) 97.
[14] S.K. Kurtz, T.T. Perry, J. Appl. Phys. 39 (1968) 3798.
[15] J.J. Shyu, J.R. Wang, J. Am. Ceram. Soc. 83 (2000) 3135.
[16] A.R. Kortan, N. Kopylov, B.I. Greene, A.M. Glass, J. Mater. Res. 17 (2002) 1208.
[17] J.T. Shiue, T.T. Fang, J. Eur. Ceram. Soc. 22 (2002) 1705.
[18] A.M. Glass, J. Appl. Phys. 40 (1969) 4699.
[19] Y. Xu, C.J. Chen, R. Xu, J.D. Mackenzie, Phys. Rev. B 44 (1991) 35.
[20] Y.Y. Zhu, J.S. Fu, R.F. Xiao, G.K. Wong, Appl. Phys. Lett. 70 (1997) 1793.
[21] L.I. Ivleva, T.R. Volk, D.V. Isakov, V.V. Gladkii, N.M. Polazkov, P.A. Lykov, J. Cryst. Growth 237–239 (2002) 700.
[22] K. Masuno, J. Phys. Soc. Jpn. 19 (1964) 323.
[23] N. Wakiya, J.K. Wang, A. Saiki, K. Shinozaki, N. Mizutani, J. Eur. Ceram. Soc. 19 (1999) 1071.
[24] W. Sakamoto, M. Mizuno, T. Yamaguchi, K. Kikuta, S. Hirano, Jpn. J. Appl. Phys. 42 (2003) 5913.
[25] T. Volk, L. Ivleva, P. Lykov, N. Polozkov, V. Salobutin, R. Pankrath, M. Wohlecke, Opt. Mater. 18 (2001) 179.
[26] M. Sato, T. Komatsu, unpublished data.
[27] E. Amazallag, T.S. Chang, R.H. Pantell, R.S. Feigelson, J. Appl. Phys. 42 (1971) 3254.
[28] M.M.T. Ho, C.L. Mak, K.H. Wong, J. Eur. Ceram. Soc. 19 (1999) 1115.
[29] S.G. Lu, C.L. Mak, K.H. Wong, J. Am. Ceram. Soc. 86 (2003) 1333.
[30] A. Kumar, D.K. Rai, S.B. Rai, Spectrochim. Acta A 59 (2003) 917.
[31] V.C. Costa, Y. Shen, A.M.M. Santos, K.L. Bray, J. Non-Cryst. Solids 304 (2003) 238.
[32] J.J. Romero, D. Jaque, L.E. Bausa, A.A. Kaminskii, J.G. Sole, J. Lumin. 87–89 (2000) 877.
[33] T. Woike, V. Petricek, M. Dusek, N.K. Hansen, P. Fertey, C. Lecomte, A. Arakcheeva, G. Chapuis, M. Imlau, R. Pankrath, Acta Crystallogr. B 59 (2003) 28.